7500 J. Phys. Chem. A **2005,** *109,* 7500−7508

On the Nature of Metal−Carbon Bonding: AIM and ELF Analyses of MCH_n ($n = 1-3$) Compounds Containing Early Transition Metals

Isaac Vidal, Santiago Melchor, and José A. Dobado*

Grupo de Modelización y Diseño Molecular, Departamento de Química Orgánica, Facultad de Ciencias, Universidad de Granada, Granada, E-18071, Spain

Received: January 10, 2005; In Final Form: June 28, 2005

Ab initio and DFT calculations have been performed on a series of organometallic compounds, according to the formula MCH_n, where M = K, Ca, Sc, Ti, V, Cr, or Mn and $n = 1-3$. Various theoretical methods are compared, the B3LYP level yielding the same agreement with the experimental geometries available as the correlated MP2 and CISD methods, with the 6-311++G(3df,2p) basis set for C and H and Wachter's (15s11p6d3f1g)/[10s7p4d3f1g] basis set for transition metals. The main geometric and electronic features of the molecules studied are described, analyzing the M−C bonding characteristics in terms of the atoms in molecules theory (AIM) and the electron localization function (ELF). Although multiple bonding is expected from the Lewis bonding scheme, the results indicate an almost pure ionic bond for all of the systems studied. The net charge transfer from the metal to the carbon atom ranges from 0.5 to 1 e^-, and the electronic structure of the CH_n^- moiety is unaltered after the interaction with the metal cation, showing little or no effect on the shape of the electron pairing. The bond paths corresponding to a possible α-agostic bond for these systems are not present.

Introduction

Organometallic compounds play a key role in various fields of chemistry, including homogeneous and heterogeneous catalysis,[1,2] polymerization,[3] and relevant biological processes.[4] In the last few decades, large advances have been achieved in the synthesis of transition-metal carbenes[5,6] and carbynes[7] and their application in synthesis, such as olefin metathesis.[8] For these compounds, the most characteristic feature is the interaction of carbon with the metal, which shows different energetic and electronic properties[7,9] depending on the ligand attached to the carbon atom (Fischer[10] and Schrock[11] types). Most theoretical studies performed previously on the nature of M−C bonds rely on geometric parameters, vibrational modes,[12−15] or molecular orbital (MO) analyses[5] instead of using a well-defined physical observable such as the electron density. From these MO analyses, the bonding scheme is defined as a consequence of an interaction between the p and d orbitals of the carbon and metal atoms, respectively,[16−18] but this does not explain the high polarization and charge transfer between the metal and the carbon, which points to a mostly ionic bond.

Although many theoretical studies are reported in the literature,[19−29] and experimental data is also available,[30−36] a general topological analysis of their electronic structure is required to describe correctly the nature of the interaction between the carbon and the transition metal. Therefore, in the current study we perform a comparative characterization of the M−C bonding in model systems that are assumed to have standard triple, double, and single bonds from a classical Lewis scheme, corresponding to the general formula MCH_n, where $n = 1-3$, respectively (Scheme 1). The metals were chosen with atomic numbers ranging from 19 to 25, allowing a direct comparison between standard ionic bonds with K or Ca, and those with early first-row transition metals, highlighting their similarities. Discrepancies in the geometry of some of these compounds still persist. In particular, two separate studies determined two different geometries for the ground state of $TiCH_2$, with C_{2v} and C_s symmetries.[25,27]

SCHEME 1: Different Conformations for the Studied Methylidynes, MCH, Methylidenes, MCH_2, and Methyl−Metals, MCH_3

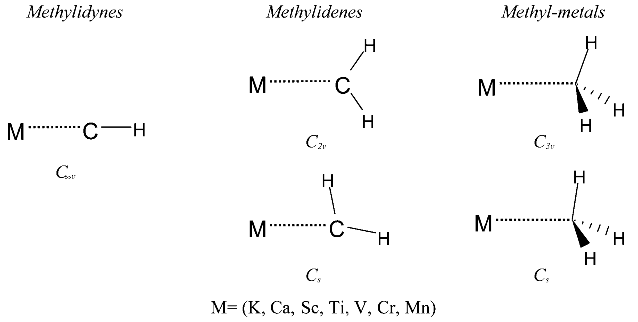

One of our main goals consists of a comparative and systematic description of the primary characteristics of the electronic structure of these compounds within the framework of the atoms in molecules theory (AIM)[37−39] in order to describe the interaction between the carbon and the transition-metal atoms. Apart from the AIM theory data, additional information about the character of the M−C bond can be extracted from the analysis of the electron pairing in the molecule. Electron pairing can be visualized adequately via the electron localization function (ELF),[40] allowing the measure of the spatial distribution and the number of paired electrons. Within this framework, a complete set of topological tools has been applied successfully for the determination of the bonding nature in many systems.[41−46]

In the past few years there have been several studies on the bonding nature of transition metals, based on topological analyses of the electron density.[47] These analyses can distin-

---

* Corresponding author. E-mail: dobado@ugr.es.

10.1021/jp050146q CCC: $30.25

guish, even under complex bonding situations, the existence or not of metal−carbon bonds[48] and have been applied to metallic clusters[49] and even to systems containing second-row transition metals, such as metal−metal bonds[50] or metals adsorbed on oxide surfaces.[51] It is remarkable that a correlation between bond distance and delocalization indices has been found,[50] challenging the interpretations based on the standard MO picture that yields bond orders ranging from 0 to 4. The bond nature is identified readily within the AIM and ELF analysis. Particularly, ELF topological analysis provides insight into the bond order,[40,50,52−54] and it has also been applied to characterize hydrogen bonds[55] and bonds formed with rare-gas atoms.[56]

For complexes containing transition metals, electron correlation has to be accounted adequately. This can be accomplished in several ways: DFT methods have been demonstrated to be useful in the studies of similar systems[44,57−63] and are of wide applicability in larger systems because of their lower computational cost. For corroboration of the DFT results, other methodologies accounting the electron correlation, such as MP2,[64] and CISD[65] methods are employed here. In the present work we also use several basis sets, including the m6-31G*[66] and others with higher variational flexibility, such as Wachters and Hay[67] and Bauschlicher[68] basis sets.

Therefore, the goal of this work is the complete and systematic analysis of the geometries of a whole family of small organometallic compounds, the characterization of their electronic structure in terms of the electron distribution and pairing, and the description of the potential energy surface for these molecules, to determine whether the M−C bond can be considered multiple.

Methodology

All of the calculations were performed with the Gaussian 03[69] software package. Different methodologies were employed to test the reliability of the calculations and the reproduction of the experimental data available. These include DFT and post-Hartree−Fock procedures, the widely accepted Becke's three-parameter hybrid functional B3LYP,[70] the second-order corrected MP2 method,[64] and the configuration interaction method with single and double excitations CISD.[65]

Although more precise methodologies can be used over these systems,[71,72] it has been demonstrated that methods based on single-determinants are adequate for the reproduction of experimental data, especially the DFT methods,[57] including pure[59,60] and hybrid[58,60−62,73] functionals. These methods have been applied to determine binding energies[61] and to characterize catalytic processes[59] and reactivity[61] in systems containing transition metals. Some of the systems studied include bonds between metal and nitrogen group atoms,[60] second-row transition metals,[63] and even organolanthanide compounds.[62] Their performance has been compared with MRCI calculations for all first-row transition-metal monocarbides and monoxides,[57] leading to a similar accuracy for B3LYP and MRCI methodologies.

Four combinations of basis sets with different variational flexibility were compared (called BS1−BS4) in order to select the most adequate one in terms of reliability and computational cost. The basis set chosen ranged from simple double-ζ basis sets to more extended Bauschlicher basis sets. This includes the specially parametrized m6-31G*[66] for transition metals, the extended Pople's 6-311++G**,[74] and those developed by Wachters and Hay[67] and Bauschlicher.[68] The BS1 set, designed for low computational cost for transition metals uses m6-31G* basis set,[66] of the form (22s16p4d1f)/[5s4p2d1f], giving a balanced description of C and H, with the 6-311++G** basis set. The BS2 basis set, coded under Gaussian 03 as 6-311++G**, also employs the Pople's 6-311++G** basis set for C and H, whereas for transition-metal atoms the Wachters−Hay[67] one is used (15s11p6d1f)/[10s7p4d1f] and for K and Ca (15s12p4d)/[9s8p2d] is used. The BS3 basis set, labeled in Gaussian 03 as 6-311++G(3df,2p), adds extra polarization functions to BS2, thus using 6-311++G(3df,2p) for C and H, and adding 2f and g functions for the metal atoms, and extra 2d and f functions for K and Ca. Finally, the BS4 refers to Dunning's[75] aug-cc-PVQZ basis set for C and H, and the much more accurate Bauschlicher basis set for transition-metal atoms, (21s16p9d6f4g) for Sc and Ti, and (20s15p10d6f4g) for V, Cr, and Mn, contracted to [7s6p4d3f2g].

Because of the highly unoccupied d shell of early first-row transition metals, their electrons are allowed to remain unpaired, and therefore the spin multiplicity of the molecule cannot be determined a priori. For its correct determination, various multiplicities were explored for each compound, ranging up to the octet state for Mn compounds. All of the structures were fully optimized for each methodology employed, and the nature of the stationary points were determined through the Hessian matrix of second derivatives (normal-mode frequency calculation), finding true minima with no imaginary frequencies for all of the structures. For each molecule, two different geometries were explored on their PES (see Scheme 1) corresponding to high and low symmetry structures, the latter presenting a hydrogen atom closer to the metal atom. Because of the different symmetries of methylidynes, methylidenes, and methyl−metals, we measure the rocking of the CH_n group with an angle γ defined in such manner that is comparable for all of them. Bending angle γ is 180° for straight structures (with C_∞, C_{2v}, and C_{3v} symmetries, respectively) and reduces as the rocking increases, leading to C_s symmetric structures. For details on its definition, see the Supporting Information (Figure S-1)

The electronic structure resulting from the calculations was analyzed in terms of the AIM theory[37−39] and, complementarily, through the distribution of the electron localization function. This function was first introduced by Becke and Edgecombe[76] and reinterpreted by Silvi and Savin[40] as a measure of the excess of local kinetic energy due to Pauli's exclusion principle, in comparison to a uniform electron gas. The ELF definition, which is found elsewhere,[40] yields values between 0 and 1. Values close to 1 indicate electron pairing at that point, whereas values near 0 are usually found in regions between electron pairs. As in AIM analysis, it is possible to divide the molecular domain in basins grouped around the ELF attractors. From a chemical standpoint, basins can be classified as being of core, valence, or hydrogenated. If the basin does not contain a nuclei, it is called a valence basin, whereas if it contains a nucleus other than a proton it is called a core basin, or hydrogenated if a proton is inside the basin. Valence basins are characterized by the number of core basins with which they are connected and this is known as the synaptic order.[77]

Other parameters also employed here for the characterization of the M−C bond are the delocalization indices and the Jansen indices. The delocalization index δ(A, B) provides a quantification of the total Fermi correlation between two basins, corresponding to the number of shared electron pairs between basins A and B. In addition, a quantification of a chemical concept such as bond polarity can be derived from both AIM theory and the ELF. Combining the partitioning of the molecular space in AIM and ELF basins, it is possible to establish a measure of how the bond is polarized toward a particular atom. As pointed out by Jansen,[78] bond polarity can be measured with the

TABLE 1: Selected Geometrical Parameters and Electronic AIM and ELF Data for Methylidynes at Their Ground State ($C_{\infty v}$) Calculated at the B3LYP/BS3 Level[a]

	KCH	CaCH	ScCH	TiCH	VCH	CrCH	MnCH
electronic state	$^3\Sigma^-$	$^4\Sigma^-$	$^3\Pi$	$^2\Sigma^+$	$^3\Delta$	$^4\Sigma^-$	$^3\Delta$
M−C (Å)	2.523	2.445	1.893	1.686	1.697	1.752	1.743
M−C (Å) exptl	2.530[b]			1.728[c]	1.703[d]		
ω_s (cm^{-1})	384	463	797	945	701	624	597
μ (D)	8.19	3.67	3.17	3.00	2.90	3.15	3.11
D_0 (kcal/mol)	47.2	44.34	89.4	106.4	101.4	82.8	44.5
$\rho(r)$ ($e{\cdot}a_0^{-3}$)	0.030	0.035	0.139	0.203	0.203	0.174	0.172
$\nabla^2\rho(r)$ ($e{\cdot}a_0^{-5}$)	0.111	0.166	0.336	0.444	0.428	0.412	0.441
ϵ	0.000	0.000	0.569	0.000	0.000	0.000	0.000
E_d (hartree$\cdot a_0^{-3}$)	0.003	0.003	−0.062	−0.148	−0.139	−0.100	−0.095
δ(M, C)	0.30	0.30	1.60	2.70	2.30	1.80	1.80
Q_M (e$^-$)	0.8	0.9	1.0	0.9	0.8	0.6	0.6
$J_{(M-C)}$ (%)	2.40	3.12	9.31	19.05	15.38	18.25	14.58

[a] See methodological section for definitions. Carbon−metal bond distances, M−C, stretching-mode frequencies, ω_s, dipole moments, μ, dissociation energies, D_0, electron density, $\rho(r)$, its Laplacian, $\nabla^2\rho(r)$, ellipticities, ϵ, and electron energy density $E_d(r)$ calculated at the BCP, M−C delocalization indices δ(C, M), electron charges integrated over the metal basin Q_M, and the Jansen indices, $J_{(M,C)}$ [b] See ref 30. [c] See ref 33. [d] See ref 34.

percentage of valence-bonding ELF basin placed between the C and M atoms (M−C) that is contained in the metal AIM basin. This index is known as the Jansen index, $J_{(M-C)}$. A covalent nonpolarized bond can be detected if the bonding ELF basin is distributed equally between two AIM atomic basins, with a Jansen index near 50%, whereas a prototypical ionic bond can be characterized by an ELF basin being almost contained in one of the two AIM atomic basins forming the bond.

The AIM and ELF analyses were carried out from the computed B3LYP/BS3//B3LYP/BS3 electron density, with the AIMPAC[79] and ToPMoD[80] software packages, respectively. Jansen indices are also extracted from the ToPMoD output, and the $\nabla^2\rho(r)$ plots were produced with the MORPHY98 software.[81]

Results and Discussion

In the first stage of the investigation, a comparison between the different method/basis set combinations and the experimental data available was made in order to test the methodologies employed and to find the best one to be applied. The geometric data calculated at these computational levels for KCH, TiCH, CrCH, VCH_2, KCH_3, and $CaCH_3$ are compared with the experimental data in the Supporting Information (Table S-2). The calculated bond distances vary with the theoretical level, but the differences due to the basis set size are less significant. Overall, the BS1 basis set yields intermediate M−C bond distances between those calculated with the BS2 and BS3 basis sets, or even lower than those obtained with BS3. Generally, the differences between the BS1 and BS3 basis sets resulted in small differences in bond distances (about 0.01 Å), although considerable gaps appeared under specific circumstances. Therefore, it can be deduced that although the BS1, using the m6-31G* basis set, is the smallest one in this work, its quality is comparable to BS3, although it may provide inaccurate geometries. Additionally, the larger BS4 basis set yields almost the same bond distances as BS3 at the B3LYP and CISD levels. This and the huge computational resources needed for the BS4 basis set (about 60 times higher in CPU time) resulted in choosing BS3 for the remaining investigation.

A. Methylidyne Compounds (MCH). The optimized structures for all methylidynes belong to the $C_{\infty v}$ and agree with the experimental values available, with differences smaller than 0.007 Å for KCH and VCH but presenting a pronounced deviation of 0.04 Å for TiCH. This particular structure has been calculated previously at higher correlated levels, providing a better agreement.[26] Nevertheless, these data will allow a discussion of their differences in terms of the electronic structure. Table 1 summarizes the main geometrical data, together with selected electronic properties from the AIM and ELF analyses.

The AIM analysis indicates that $\rho(r)$ for the M−C BCP is relatively low for these compounds, where a triple bond is expected, being in the 0.17−0.20 $e{\cdot}a_0^{-3}$ range for all early transition metals. The $\rho(r)$ values increase rapidly from KCH to TiCH with the atomic number, reaching a maximum for TiCH, and decrease slowly after it. The $\nabla^2\rho(r)$ values at the BCP's are always positive and indicate a clear ionic character of all of the methylidyne compounds. These $\nabla^2\rho(r)$ values follow the same trend as the $\rho(r)$ ones, increasing from KCH to TiCH and remaining almost constant beyond TiCH. The charge dispersion is higher for transition metals, indicating a strong charge depletion around the BCP and a sharp decrease in the electron density when crossing the interatomic surface between M and C atoms.

Although these bonds are ionic, not all of the bonds showed an isotropic electron distribution at the BCP, as would have been expected, but rather some ellipticity values were nonzero. In particular, ScCH showed an abnormally high ϵ value, which will be explained below. Additional information on the nature of the M−C interaction is provided by the electron energy density, $E_d(r)$, and the delocalization indices, δ(M, C), also listed in Table 1. For KCH and CaCH, $E_d(r)$ values are positive and very low. On the contrary, for the early transition metals, $E_d(r)$ is negative, evidencing the excess of electron kinetic energy at the BCP and therefore how the M−C interaction stabilizes the whole system, when compared to the M−C bonding in KCH and CaCH. Additionally, δ(M, C) values are always greater than 1.5 for transition-metal derivatives, indicating a higher electron sharing between M and C basins, and thus a higher covalent character in the M−C bond. Nevertheless, the δ(M, C) values should be considered carefully in order to avoid misunderstanding: following recent interpretations,[82] the δ(X, Y) values for those bonds presenting charge transfer cannot be interpreted as the Lewis bond order but rather as the number of electrons shared between two atoms. These concepts coincide in homopolar bonds, but when the electrons participating in the bond are very unequally shared, approaching the ionic limit, this is not true. Nevertheless, both $E_d(r)$ and δ(M, C) present the same trend as $\rho(r)$ and $\nabla^2\rho(r)$: minimum, almost zero values were found for KCH and CaCH, increasing rapidly from ScCH to

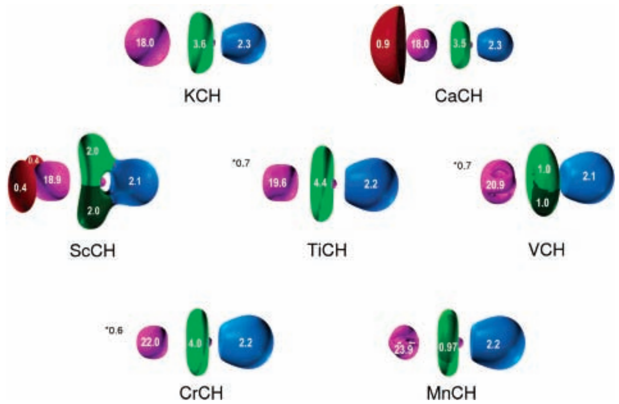

Figure 1. ELF isosurfaces and electron-pairing basin populations for the MCH overall minima, computed at a value of 0.75, except for ScCH, which is displayed with a 0.65 value in order to show the two monosynaptic basins. Asterisks denote the existence and the population of basins with ELF values below 0.75. The color convention represents core basins in magenta, and the remaining valence basins are classified depending on the number of connections to core nuclear basins (synaptic order): red for monosynaptic, green for disynaptic, and cyan for disynaptic hydrogenated basins.

TiCH, where maximum values were found, and then a slow decrease for higher atomic numbers.

The AIM charge at the metal atom (Q_M) for these molecules indicates clearly that, in all compounds, there is always a charge transfer of about 1 e^- from the metal to the carbon atom, although this was slightly and progressively reduced as the atomic number increased, being minimum for MnCH and CrCH (0.6 e^-).

Figure 1 shows the spatial distribution of the ELF for all methylidynes, together with the basin population values. The overall inspection of their ELF basins reveals that most of them share the same distribution, consisting of a core basin for the metallic atom, which adopts spherical and structured shapes (depending on the d shell occupation), a toroidal basin, the center of which is located very close to the carbon atomic position, and the hydrogenated basin. Eventually, external monosynaptic valence basins may appear around the metal-core basin, corresponding to unpaired electrons.

The comparison of the electron pairing present in the studied molecules, with that of the isolated anion CH^- or the neutral radical CH, provides extra information about the bond characteristics in MCH compounds, as will similar comparisons for MCH_2 and MCH_3. For this purpose, the ELF isosurfaces of CH^-, CH, CH_2^-, CH_2, CH_3^-, and CH_3 have been computed and are provided as Supporting Information (Figure S-3). To determine the nature of the interaction that takes place in MCH_n compounds, both low and high spin states were considered.

In most cases, the toroidal basin around the C atom was found to present a very similar structure to that of CH^- at the triplet state, except for ScCH. This arrangement suggests that these molecules are formed by the electrostatic interaction between M^+ and CH^- fragments. The toroidal shape presents slight modifications in its shape and population, but its position in all cases remains unaltered. The only noticeable differences in the structure of the toroidal basin were observed for VCH and MnCH, where it appears divided into four fragments of equal population. This is caused by a significant change of shape of the Cr and Mn core basins, which breaks the relatively unstable circular attractor that appears in every toroidal ELF basin.

In accordance with this idea, a toroidal M−C basin populated with 4 e^- indicates the presence of two unpaired electrons located there. Additionally, if the metal cation, resulting from transferring an electron to the CH unit, presents an odd number of electrons, the number of unpaired electrons in the whole system would be three. This results in alternated triplet and quartet spin multiplicities as the atomic number increases, except for the ScCH, where no toroidal basin appears, and TiCH. The latter presents a remarkably different population of 4.4 e^- for the M−C electron-pairing basin, together with its double spin multiplicity. This reveals that, although ionic, its bond presents the most covalent character of all bonds studied in this work. This is also confirmed by the largest $\rho(r)$ and $E_d(r)$ values, as well as the greatest delocalization and Jansen indices, revealing that this highly populated basin is shared partially between the M and C atoms by about 20%.

The situation was different for ScCH, where two separate basins with a population of 2.0 e^- synaptically connected to the M and C core basins are located at both sides of the bond, but appearing very close to the carbon nucleus. This arrangement closely resembles that of the CH^- at the singlet excited state. The reasons that compound ScCH differs in its electronic structure can be found in the spatial localization of the unpaired electrons. For ScCH, the triplet characteristics are located at the metal center, presenting two unpaired electrons that tend to repel each other maximally. This is noticed in the presence of two separate ELF basins with an ELF value slightly higher than 0.65. Their population is of 0.4 e^- each, this magnitude not accounting for the whole population of the two unpaired electrons, because ELF does not describe unpaired electrons correctly. The arrangement of these unpaired electrons is incompatible with the toroidal shape for the four electrons located between M and C, thus favoring the singlet state for the CH^- moiety instead of its triplet ground state. The CH^- singlet state presents two pairing basins with 2 e^- each, which in ScCH appear perpendicularly to both external ELF basins of Sc^+. Therefore, it may be concluded that the interaction between M^+ and CH^- moieties is the result of excitation from the CH^- triplet to the singlet state, which is reflected in a very low triplet−singlet excitation energy (5.3 kcal/mol for ScCH). This situation is possible only if the number of unpaired electrons in the metal is two, as in ScCH. This difference in the bonding for ScCH, and more specifically in the electron-pairing distribution around the carbon atom, results in an anisotropy for the electron density in the regions between the metal and the carbon, causing the abnormally high ellipticity value in the Sc−C BCP. The Jansen indices for methylidynes are also listed in Table 1 and indicate that the percentage of the M−C ELF basin that belongs to the metal atomic basin is minimal for K and Ca and is always below 20%.

B. Methylidene Compounds (MCH_2). Some of these compounds have been studied theoretically elsewhere,[19,25,27,29] but there are some discrepancies concerning their reported symmetries. For example, the structure of $TiCH_2$ is questioned in two different studies. Sosa et al. found C_{2v} symmetry[27] for $TiCH_2$, whereas Dalmazio et al. assigned it to the C_s point group.[25] Therefore, special attention will be paid here to the geometry of $TiCH_2$. A similar study of $ScCH_2^+$ and $TiCH_2^+$ cations by Ricca et al.[73] at various levels of theory (B3LYP, CCSD(T), and CASSCF) also found the bent C_s structure as the global minimum instead of the C_{2v} one, where the energy difference between C_s and C_{2v} geometries is less than 2 kcal/mol. This highlights the special behavior of Sc and Ti atoms. The geometry of $TiCH_2^+$ was also undetermined in that work, as CASSCF methodology found the C_{2v} structure to be a relative minimum with no imaginary frequencies, whereas other theoretical levels revealed it to be a transition state.[73] These results

TABLE 2: Selected Geometrical Parameters and Electronic AIM and ELF Data for Methylidenes at Their Ground State, Calculated at the B3LYP/BS3 Level[a]

	KCH_2	$CaCH_2$	$ScCH_2$	$TiCH_2$		VCH_2	$CrCH_2$	$MnCH_2$
symmetry	C_{2v}	C_{2v}	C_s	C_s	C_{2v}	C_{2v}	C_{2v}	C_{2v}
electronic state	$^2B_1$	$^3B_1$	$^2A'$	$^3A'$	$^3B_2$	$^4B_2$	$^5B_1$	$^4A_2$
M−C (°)	2.590	2.318	1.880	1.824	1.881	1.893	1.910	1.907
M−C (°) exptl							1.9[b]	
γ (°)	180	180	142.3	142.8	180	180	180	180
∠HCH (°)	105.3	106.8	111.4	112.9	111.2	111.9	112.7	113.4
ω_s (cm^{-1})	342	466			584	537	541	552
μ (D)	7.77	2.14	3.48	2.88	2.51	2.45	2.63	2.30
D_0 (kcal/mol)	36.2	35.1	81.0	86.4	74.2	88.0	66.5	52.3
$\rho(r)$ ($e{\cdot}a_0^{-3}$)	0.034	0.060	0.149	0.166	0.153	0.144	0.134	0.136
$\nabla^2\rho(r)$ ($e{\cdot}a_0^{-5}$)	0.109	0.166	0.229	0.213	0.242	0.232	0.232	0.224
ϵ	0.081	0.107	0.586	0.487	0.331	0.267	0.224	0.193
E_d (hartree$\cdot a_0^{-3}$)	0.000	−0.006	−0.075	−0.095	−0.080	−0.071	−0.059	−0.058
δ(M,C)	0.4	0.5	1.7	1.6	1.6	1.4	1.2	1.0
Q_M (e^-)	0.7	0.8	0.9	0.8	0.8	0.6	0.6	0.5
$J_{(M-C)}$ (%)	3.7	5.5	10.8	15.7	17.0	16.2	16.8	15.6

[a] See methodological section for definitions. Carbon−metal bond distances, M−C, bending angles, γ, ∠HCH angles, stretching-mode frequencies, ω_s, dipole moments, μ, dissociation energies, D_0, electron density, $\rho(r)$, its Laplacian, $\nabla^2\rho(r)$, ellipticities, E, and electron energy density, $E_d(r)$, calculated at the BCP, M−C delocalization indices δ(C, M), electron charges integrated over the metal basin, Q_M, and the Jansen indices, $J_{(M,C)}$ [b] See ref 35.

indicate the great importance of the level used in the determination of the geometric characteristics for these compounds.

The geometrical parameters of the overall minima for methylidenes are listed in Table 2 along with parameters related to their electronic structure. Similar to the results of Ricca et al.,[73] $ScCH_2$ and $TiCH_2$ have C_s geometries with one of the H atoms oriented toward the metal, yielding γ angles of 143.2° and 142.8°, respectively, but 180° for the rest of the molecules. Comparison between calculated and experimental values is only possible for $CrCH_2$. Although Cr−C distances show considerable experimental uncertainty, the agreement with the calculated bond distances can be considered acceptable. The experimental ∠HCH angle of 113° is in perfect agreement with our calculated value of 112.7°.

For all of the methylidene compounds, the C−H bond distance is almost unaffected by the coordinated metal, remaining in a narrow 1.09−1.10 Å range, except for the $ScCH_2$ and $TiCH_2$ molecules, which present differentiated C−H bonds. Only a slight and progressive C−H bond length reduction from KCH_2 to $MnCH_2$ is observed. In addition, the ∠HCH angle is in a 111−113° narrow range for transition metals and about 107° for KCH_2 and $CaCH_2$. It is interesting that even for the $ScCH_2$ and $TiCH_2$ distorted geometries, this ∠HCH angle remains in the same range.

The integrated charges over the atomic basins indicate that the charge transfer from the metal to the carbon is again almost constant, being about 0.8 e^- from KCH_2 to $TiCH_2$, and then reduces progressively to 0.5 e^- in $MnCH_2$. The AIM and ELF data measured at the BCP showed behavior similar to that of the methylidynes, in the sense that $\rho(r)$ values are small, and the Laplacian clearly indicates the ionic character of the bond, although a slight degree of covalent character can be detected in the negative values (stronger for Ti and Sc compounds) of $E_d(r)$. The ϵ values are low for KCH_2 and $CaCH_2$, whereas $ScCH_2$ and $TiCH_2$ show the greatest anisotropy. Jansen indices also clearly point to the M−C ionic bond character in all methylidenes. The metal AIM contribution to the ELF bonding basin hardly reaches 17%, the remaining 83% belonging to the carbon atom. In Figure 2, the differences in the ELF distribution between alkali and alkali-earth with the transition-metal compounds are more pronounced. For these, the CH_2 group best matched the shape of the CH_2^- anion at the doublet state, (See Supporting Information Figure S-3) characterized by an elongated carbon-valence basin with a population close to 3 e^-; thus, the unpaired electron is localized in that basin. Although a certain degree of asymmetry can be seen in this basin's shape, it is organized around a single attractor for KCH_2 and $CaCH_2$, in a way similar to the CH_2^- anion. On the contrary, the early transition-metal compounds present a M−C basin that still contains three electrons, but is clearly divided in two, presumably induced by the presence of the metal, also indicating a higher degree of covalent character. The population of this basin decreases from 3.2 to 2.6 e^-, as the metal atomic number increases, in accordance with the decrease in the above-mentioned charge transfer.

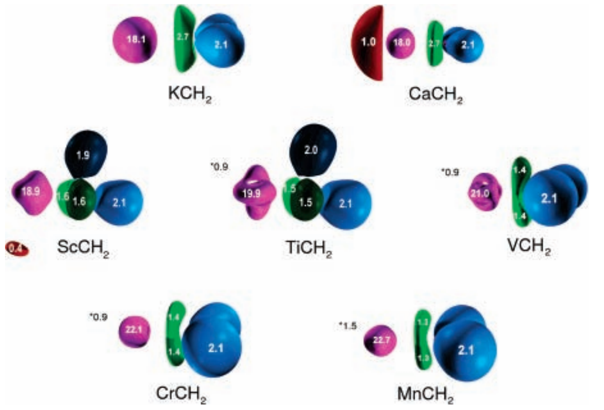

Figure 2. ELF isosurfaces and electron-pairing basin populations for the MCH_2 overall minima, computed at a value of 0.75. Asterisks denote the existence and the population of basins with ELF values below 0.75. See Figure 1 caption for the color convention.

The readily visible geometric differences presented in $ScCH_2$ and $TiCH_2$ with respect to the linear structures are not reflected in the ELF pairing distribution, as might be expected. The electronic structure of the CH_2 moiety remains almost the same for all of the transition-metal methylidenes, and only their pairing basins are displaced together around the carbon p_z axis. The change in the geometry is reflected merely in a very slight distinction between both C−H bonds, such as in their bond lengths and in the ELF basin population, caused by the proximity

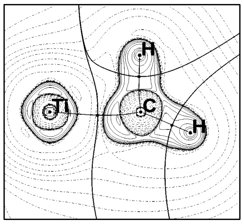

Figure 3. Laplacian $\nabla^2\rho(r)$ contour maps, in the molecular structure of $TiCH_2$ computed at the B3LYP/6-311++G(3df,2p) level. The contour values correspond to ±0.02, ±0.04, ±0.08, ±0.2, ±0.4, ±0.8, ±2.0, ±4.0, and ±8.0 $e{\cdot}a_0^{-5}$, where the dashed lines indicate negative values.

of one H atom to the metal atom, resulting in its bond lengthening and a decrease in the hydrogenated ELF basin population.

From the geometrical standpoint, the proximity of the M and H atoms can be considered to be an α-agostic bond,[83] but this needs to be examined thoroughly. For that purpose, Figure 3 plots the diagram of the Laplacian, together with the interatomic surfaces (thick lines) for $TiCH_2$. The $\nabla^2\rho(r)$ plots for all of the compounds studied in this work is provided as Supporting Information (Figure S-4). The corresponding C−H and M−C surfaces get asymptotically closer to each other, but there is no BCP connecting them. This indicates that there is no surface shared between the M and H basins, and therefore, no α-agostic bonding was detected. Similar behavior was also found for $ScCH_2$.

Once the presence of an α-agostic bond linking both M and H atoms has been ruled out, the approach between the metal and one of the hydrogen atoms in $ScCH_2$ and $TiCH_2$ requires further investigation. For that purpose, although these compounds present geometries of lower symmetry (C_s) as their overall minima, C_{2v} relative minima were also sought. A minimum was found only for $TiCH_2$, presenting no imaginary frequencies, whereas for $ScCH_2$, on the contrary, the C_{2v} geometry constitutes a transition state. Nevertheless, the energy difference between C_s and C_{2v} structures for $TiCH_2$, is extremely low (0.55 kcal/mol). The AIM and ELF analyses revealed that the bond properties of $ScCH_2$ and $TiCH_2$ are in line with the rest of early transition-metal methylidene compounds, and no differences were found in either the electron density or the ELF basin distribution. It appears that the severe rotation of the CH_2 moiety around the carbon p_z axis has no effect on the M−C bonding characteristics. This is compatible with the idea of an ionic bond, where the Ti and Sc atoms are attracted merely electrostatically to the CH_2 unit, regardless of the relative position of the substituents.

The $TiCH_2$ geometry presents an additional characteristic feature, consisting of the elongation of the Ti−C bond distance in 0.057 Å relative to the C_s conformer. These differences can be explained considering the electronic structure of $TiCH_2$. The conformation change from C_s to C_{2v} symmetries requires the ELF valence basins for the carbon to be placed directly between the M and the C atoms.

If the bonding between M and C were covalent, then the hybrid carbon sp^2 orbital would tend to overlap maximally with those orbitals from the metal, by aligning the symmetry axis of the carbon sp^2 orbital with the metal atom. The axis orientation is noticed in the position of the substituents around carbon, leading to a bending angle, γ, of 180° when the metal nucleus is aligned with the carbon sp^2 orbital. But for $ScCH_2$ and $TiCH_2$, the metal core is not aligned, evidencing the absence of σ contribution to the M−C bonding. Even more, apart from the energetic destabilization resulting from aligning the carbon sp^2 orbital and the metal, the C_{2v} configuration with $\gamma = 180°$ results in an elongation of the M−C bond distance, indicating that the σ interaction does not contribute to the bond stability. This behavior has been investigated complementarily by exploring the potential energy surface of $TiCH_2$. Figure 4 plots the energetic destabilization resulting from the variations of the γ angle at four different Ti−C bond-length values. For Ti−C distances similar to those on the C_s conformer (1.824 Å), the curves present two equivalent minima separated by a barrier of ca. 1 kcal/mol. As the bond-length parameter increases, the minima are lifted and the barrier reduced simultaneously, up to a distance of 1.88 Å, where the curve reaches an almost planar shape from 150−210°, but with a true minimum at $\gamma = 180°$. The scattered dots in Figure 4 represent the corresponding curve with all geometric parameters fitted to that of the C_{2v} structure, yielding almost no difference. These double minima and the very planar energetic curves reflect the high instability of the C_{2v} conformer, and also the wide freedom of movement for the CH_2 group, which can rotate almost freely in a range of 80° for the γ angle, the only limitations to its movement being the relative repulsion at short-distances between the M and carbon-valence basins.

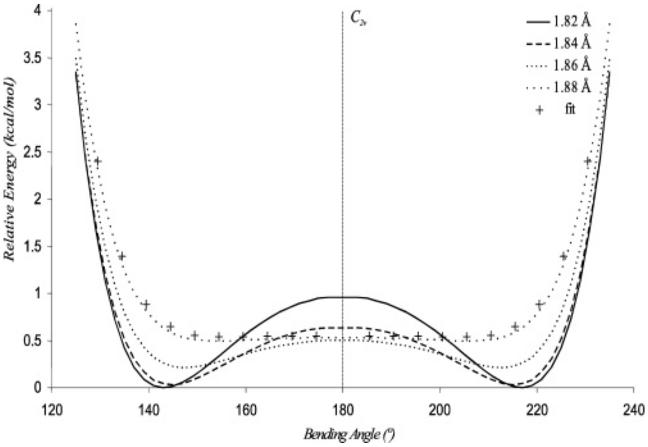

Figure 4. Energy variations of $TiCH_2$ with the bending angle γ, calculated at four different M−C bond-distance values. Scattered points indicate the variations when the remaining geometric parameters are fitted to those of the C_{2v} structure.

C. Methyl−Metal Compounds (MCH_3). Although most of these compounds have been characterized theoretically, no analysis of their electronic structure has been performed yet, and therefore they are included in this work. The previous theoretical studies report C_{3v} geometries at their ground state for all methyl−metal compounds. Table 3 lists the geometries obtained as well as data relative to the electronic structure for the optimized geometries. KCH_3, $CaCH_3$, $ScCH_3$, and $TiCH_3$ present C_{3v} symmetry, whereas for the remaining, their symmetry is reduced to C_s because of a weak rocking of the CH_3, more noticeable for $MnCH_3$. This rocking can be measured with the γ bending angle formed with the M−C bond and the pyramidalization vector of the CH_3 group (see Supporting Information Figure S-1). This results in γ values of 177.9, 175.7, and 165.8° for VCH_3, $CrCH_3$, and $MnCH_3$, respectively. Such distortion is increased progressively with the atomic number of the metal, but in all cases the piramidalization angle of the CH_3 unit is always about 70°, with an approximate dispersion range of 1°. For comparison, this angle for a pure sp^3 hybridization such as that in methane is 70.5°. This allows us to conclude that the distorted structures for methyl−metal compounds behave similar to those of the methylidene series.

TABLE 3: Selected Geometrical Parameters and Electronic AIM and ELF Data for Methyl−Metals at Their Ground State, Calculated at the B3LYP/BS3 Level[a]

	KCH_3	$CaCH_3$	$ScCH_3$	$TiCH_3$	VCH_3		$CrCH_3$		$MnCH_3$	
symmetry	C_{3v}	C_{3v}	C_{3v}	C_{3v}	C_s	C_{3v}	C_s	C_{3v}	C_s	C_{3v}
electronic state	$^1A_1$	$^2A_1$	$^1A_1$	$^4A_1$	$^3A''$	$^3A_1$	$^4A'$	$^4A_1$	$^3A''$	$^3A_1$
M−C (Å)	2.671	2.357	2.107	2.126	2.063	2.035	2.025	2.029	1.958	2.050
M−C (Å) exptl	2.633[b]	2.349[c]								
γ (°)	180.0	180.0	180.0	180.0	177.9	180.0	175.7	180.0	165.8	180.0
POAV1 (°)	69.0	67.9	70.3	69.2	70.2	71.2	71.1	70.8	70.7	68.7
ω_s (cm^{-1})	290	415	519	482		474		478		465
μ (D)	7.12	2.40	0.85	2.02	1.30	0.80	0.96	0.95	1.75	2.73
D_0 (kcal/mol)	23.19	20.9	50.3	58.7	38.9	35.9	7.7	2.3	−29.7	−37.2
$\rho(r)$ ($e{\cdot}a_0^{-3}$)	0.031	0.060	0.113	0.097	0.110	0.120	0.116	0.114	0.123	0.088
$\nabla^2\rho(r)$ ($e{\cdot}a_0^{-5}$)	0.085	0.117	0.024	0.101	0.087	0.063	0.095	0.109	0.155	0.286
e	0.000	0.000	0.000	0.000	0.255	0.000	0.179	0.000	0.490	0.000
E_d (hartree$\cdot a_0^{-3}$)	0.000	−0.007	−0.050	−0.035	−0.043	−0.050	−0.045	−0.043	−0.049	−0.025
δ(M, C)	0.4	0.5	0.9	0.8	0.9	1.0	0.9	1.0	1.1	1.0
Q_M (e$^-$)	0.6	0.5	0.6	0.6	0.5	0.5	0.6	0.4	0.4	0.5
$J_{(M-C)}$ (%)	7.0	8.1	11.2	11.3	13.7	12.8	14.6	17.9	22.1	28.3

[a] See methodological section for definitions. Carbon−metal bond distances, M−C, bending angles, γ, pyramidalization angles, POAV1, stretching-mode frequencies, ω_s, dipole moments, μ, dissociation energies, D_0, electron density, $\rho(r)$, its Laplacian, $\nabla^2\rho(r)$, ellipticity, *E*, and electron energy density, $E_d(r)$ measured at the BCP, M−C delocalization indices δ(C, M), electron charges integrated over the metal basin Q_M, and the Jansen indices, $J_{(M,C)}$ [b] See ref 33. [c] See ref 34.

The CH_3 moiety preserves an almost perfect tetrahedral geometric configuration, with pyramidalization deviations of less than 0.5°.

The distortion in VCH_3 and $CrCH_3$ was small, and therefore the energetic differences with respect to the C_{3v} structures are also small, about 2.4 and 5.3 kcal/mol, respectively, for VCH_3 and $CrCH_3$. For $MnCH_3$, the differences are more pronounced, resulting to an energy difference of 7.4 kcal/mol. Nevertheless, all of the C_{3v} geometries constitute real minima without imaginary frequencies. The geometric and electronic characteristics of these C_{3v} geometries are also listed in Table 3.

The AIM parameters corresponding to the M−C bond for all of these compounds are the less significant from all standpoints, with the lowest $\rho(r)$ values, stabilizing character and delocalization indices. The ionic character of all MCH_3 compounds is sensibly lower than that of MCH_2 and MCH, indicated with a lower net charge transfer of about half an electron, in a range between 0.4 and 0.7 e^-, and lower Jansen indices, showing that less charge is contained in the carbon atom. $\nabla^2\rho(r)$ also shows their ionic character, but to a lesser degree, with appreciably lower values.

The arrangement of ELF electron-pairing basins for MCH_3 compounds is very similar for all of them, regardless of whether they are of C_{3v} or C_s symmetries. The three hydrogenated basins and the carbon-valence basin adopt a tetrahedral configuration around the carbon atom, where the valence basin directed toward the metal contains about 1.8 e^-, presenting the same shape for all MCH_3 compounds. (see Supporting Information Figure S-5). There is a clear resemblance between the ELF distribution of MCH_3 and that of the CH_3^- singlet state, but, in comparison with the distribution for the CH_3^- anion, the M−C valence basin is much more spatially localized, and its population is slightly below 2 e^-, in accordance with the lower charge transfer. Even in the highly distorted geometry of $MnCH_3$, its ELF distribution shows almost no distortion, similar to the situation for methylidene $TiCH_2$.

Conclusions

The main electronic characteristics of methylidynes, methylidenes, and methyl−metals have been described for first-row early transition metals, together with alkali and alkali-earth compounds for comparison. Different methodologies were employed and compared with the experimental data available, concluding that the best performance was provided by the B3LYP/BS3 method. The basis set developed recently, m6-31G*, for first-row transition metals, often yields data similar to those obtained with the other basis set, but larger discrepancies arise with certain metals, such as in VCH.

The previous discrepancies about their geometry have been discussed in terms of the PES, finding planar curves that indicate the reported difficulties in finding the correct minima. It is found that these compounds show an almost free rotation of the CH_n group as a whole, especially for methylidenes MCH_2, where the CH_2 group can oscillate over a range of 80° around the carbon p_z axis.

The nature of all of the M−C bonds in methylidynes, methylidenes, and methyl−metal compounds have been demonstrated to be very similar, but in different degrees. They consistently show a clear ionic character, marked by a BCP located in the charge-dispersion zone located between the paired electrons from the metallic core and the CH_2 moiety. Also, there is a charge transfer from the metal to the carbon atom invariably larger than 0.5 e^-. This transfer is highest for methylidynes (ca. 1 e^-) and lowest for methyl−metal compounds, this difference being caused mainly by the electron vacancy on the carbon-valence shell. Nevertheless, there is always a slight distinction between K and Ca compounds and the early transition-metal derivatives: for the latter ones, the M−C bond is more stabilizing, being supported by the negative $E_d(r)$ values, larger delocalization indices, δ(M,C), and larger Jansen indices, $J_{(M-C)}$, indicating a higher degree of electron sharing between the metal and the carbon. This is no obstacle for considering these bonds as single ionic ones.

Several of the structures studied presented bent geometries $ScCH_2$, $TiCH_2$, VCH_3, $CrCH_3$, and $MnCH_2$ and therefore constitute candidates to present α-agostic bonds. This was investigated in terms of AIM and ELF analyses, and there was no evidence to support such a bonding scheme. The AIM result showed that the approach between the H and the metal atoms does not result in a BCP, whereas ELF pairing basins show the same electron-pairing distribution, shape, and population as in the other molecules. This, accompanied by a clear electronic and geometric resemblance between the CH_n moiety and the CH_n^- anion, indicates the absence of σ contribution to this bonding. This is also manifested in a great torsional flexibility of the CH_n moiety for methylidenes, this behavior being maximal for $TiCH_2$, where two different symmetries with an energy difference below 1 kcal/mol are present. From the above AIM and ELF analyses, the existence of multiple bonding is questioned for these organometallic compounds, which resemble purely ionic adducts, with a small covalent contribution.

Acknowledgment. This work was financed by the Spanish Ministerio de Ciencia y Tecnología (BQU2002-01207). I.V. acknowledges Ministerio de Ciencia y Tecnología (beca de colaboración) and Universidad de Granada (beca de iniciación a la investigación) grants, respectively. Computing time was provided by the Universidad de Granada. We are grateful to Professors R. F. W. Bader and B. Silvi for supplying us a copy of the AIMPAC and ToPMoD software packages. Mr. David Nesbitt reviewed the original English manuscript.

Supporting Information Available: Scheme and description of rocking angle γ (Figure S-1), comparative table of all combinations of methods/basis sets with the experimental data (Table S-2), ELF isosurfaces for CH_n^- anions and CH_n neutral species (Figure S-3), Laplacian plots for methylidynes, methylidenes, and methyl−metals (Figure S-4), and ELF isosurfaces for methyl−metal compounds (Figure S-5). This material is available free of charge via the Internet at http://pubs.acs.org.

References and Notes

(1) Fruhauf, H. W. *Chem. Rev.* **1997**, *97*, 523.

(2) Frenking, G.; Fröhlich, N. *Chem. Rev.* **2000**, *100*, 717.

(3) Ziegler, K.; Zink, J. I. *Angew. Chem.* **1955**, *67*, 541.

(4) Bertini, I.; Gray, H. B.; Lippard, S. J.; Valentine, J. S. *Bioinorganic Chemistry*; University Science Books, 1994.

(5) Dötz, K. H.; Fischer, H.; Hofmann, P.; Kreissl, F. R.; Schubert, U.; Weiss, K. *Transition Metal Carbene Complexes*; VCH: Weinheim, Germany, 1988.

(6) Fischer, H.; Hofmann, P.; Kreissl, R. R.; Schrock, R. R.; Schubert, U.; Weiss, K. *Carbyne Complexes*; VCH: New York, 1988.

(7) Fischer, E. O.; Kreis, G.; Kreiter, C. G.; Müller, J.; Huttner, G.; Lorenz, H. *Angew. Chem., Int. Ed. Engl.* **1973**, *12*, 564.

(8) Herndon, J. W. *Coord. Chem. Rev.* **2000**, *206*, 237.

(9) Nugent, W. A.; Mayer, J. M. *Metal−Ligand Multiple Bonds*; Wiley: New York, 1988.

(10) Maasböl, A,; Fischer, E. O. *Angew. Chem., Int. Ed. Engl.* **1964**, *3*, 580.

(11) Schrock, R. R. *J. Am. Chem. Soc.* **1974**, *96*, 6796.

(12) Dao, N. Q. *J. Organomet. Chem.* **2003**, *684*, 82.

(13) Wang, C. C.; Wang, Y.; Liu, H. J.; Lin, K. J.; Chou, L. K.; Chan, K. S. *J. Phys. Chem. A* **1997**, *101*, 8887.

(14) Manna, J.; Dallinger, R. F.; Miskowski, V. M.; Hopkins, M. D. *J. Phys. Chem. B* **2000**, *104*, 10928.

(15) Cundari, T. R.; Harvey, J. N.; Klinckman, T. R.; Fu, W. T. *Inorg. Chem.* **1999**, *38*, 5611.

(16) Ziegler, T.; Tschinke, V.; Becke, A. *J. Am. Chem. Soc.* **1987**, *109*, 1351.

(17) Vyboishchikov, S. F.; Frenking, G. *Chem.−Eur. J.* **1998**, *4*, 1428.

(18) Vyboishchikov, S. F.; Frenking, G. *Chem.−Eur. J.* **1998**, *4*, 1439.

(19) Tyerman, S. C.; Corlett, G. K.; Ellis, A. M.; Caxton, T. A. *J. Mol. Struct.: THEOCHEM* **1996**, *373*, 107.

(20) Hammadi, A. E.; Mouhtadi, M. E.; Cardy, H.; Dargelos, A. *J. Mol. Struct.: THEOCHEM* **2003**, *624*, 1.

(21) Bauschlicher, C. W.; Langhoff, S. R.; Partridge, H.; Barnes, L. A. *J. Chem. Phys.* **1989**, *91*, 2399.

(22) Brazier, C. R.; Bernath, P. F. *J. Chem. Phys.* **1989**, *91*, 4548.

(23) Barckholtz, T. A.; Powers, D. E.; Miller, T. A.; Bursten, B. E. *J. Am. Chem. Soc.* **1999**, *121*, 2576.

(24) Ortiz, J. V. *J. Chem. Phys.* **1990**, *92*, 6728.

(25) Dalmázio, I.; Duarte, H. A. *J. Chem. Phys.* **2001**, *115*, 1747.

(26) Kalemos, A.; Dunning, T. H.; Harrison, J. F.; Mavridis, A. *J. Chem. Phys.* **2003**, *119*, 3745.

(27) Sosa, R. M.; Gardiol, P.; Beltrame, G. *Int. J. Quantum Chem.* **1998**, *69*, 371.

(28) Bytheway, I.; Metha, G. F. *Chem. Phys. Lett.* **2000**, *326*, 151.

(29) Brooks, B. R.; Schaefer, H. F. *Mol. Phys.* **1977**, *34*, 193.

(30) Xin, J.; Ziurys, L. M. *J. Chem. Phys.* **1999**, *110*, 3360.

(31) Grotjahn, D. B.; Pesch, T. C.; Brewster, M. A.; Ziurys, L. M. *J. Am. Chem. Soc.* **2000**, *122*, 4735.

(32) Namiki, K. C.; Steimle, T. C. *J. Chem. Phys.* **1999**, *110*, 11309.

(33) Barnes, M.; Merer, A. J.; Metha, G. F. *J. Mol. Spectrosc.* **1997**, *181*, 168.

(34) Barnes, M.; Hajigeorgiou, P. G.; Kasrai, R.; Merer, A. J.; Metha, G. F. *J. Am. Chem. Soc.* **1995**, *117*, 2096.

(35) Billups, W. E.; Chang, S. C.; Hauge, R. H.; Margrave, J. L. *Inorg. Chem.* **1993**, *32*, 1529.

(36) Billups, W. E.; Chang, S. C.; Margrave, J. L.; Hauge, R. H. *Organometallics* **1999**, *18*, 3551.

(37) Bader, R. F. W. *Atoms in Molecules: A Quantum Theory*; Clarendon Press: Oxford, U.K., 1990.

(38) Bader, R. F. W. *Chem. Rev.* **1991**, *91*, 893.

(39) Bader, R. F. W. In *Encyclopedia of Computational Chemistry*; Schleyer, P.v. R., Ed.; Wiley: Chichester, U.K., 1998.

(40) Silvi, B.; Savin, A. *Nature* **1994**, *371*, 683.

(41) Dobado, J. A.; Martínez-García, H.; Molina, J. M.; Sundberg, M. R. *J. Am. Chem. Soc.* **1999**, *121*, 3156.

(42) Dobado, J. A.; Martínez-García, H.; Molina, J. M.; Sundberg, M. R. *J. Am. Chem. Soc*. **2000**, *122*, 1144.

(43) Sánchez-González, A.; Martínez-García, H.; Melchor, S.; Dobado, J. A. *J. Phys. Chem. A* **2004**, *108*, 9188.

(44) Pilme, J.; Silvi, B.; Alikhanni, M. E. *J. Phys. Chem. A* **2003**, *107*, 4506.

(45) Chevreau, H.; Martinsky, C.; Sevin, A.; Minot, C.; Silvi, B. *New J. Chem.* **2003**, *27*, 1049.

(46) Malcolm, N. O. J.; Gillespie, R. J.; Popelier, P. L. A. *J. Chem. Soc., Dalton Trans.* **2002**, *17*, 3333.

(47) Macchi, P.; Sironi, A. *Coord. Chem. Rev.* **2003**, *238−239*, 383.

(48) Bader, R. F. W.; Matta, C. *Inorg. Chem.* **2001**, *40*, 5603.

(49) Bersky, S.; Gutsev, G. L.; Mochena, M. D.; Andres, J. *J. Phys. Chem. A* **2004**, *108*, 6025.

(50) Llusar, R.; Beltran, A.; Andres, J.; Fuster, F.; Silvi, B. *J. Phys. Chem. A* **2001**, *105*, 9460.

(51) Gomes, J. R. B.; Illas, F.; Silvi, B. *Chem. Phys. Lett.* **2004**, *388*, 132.

(52) Grutzmacher, H.; Fassler, T. F. *Chem.−Eur. J.* **2000**, *6*, 2317.

(53) Chesnut, D. B. *Chem. Phys.* **2001**, *271*, 9.

(54) Chesnut, D. B. *Heteroat. Chem.* **2003**, *14*, 175.

(55) Fuster, F.; Silvi, B. *Theor. Chem. Acc.* **2000**, *104*, 13.

(56) Berski, S.; Latajka, Z.; Silvi, B.; Lundell, J. *J. Chem. Phys.* **2001**, *114*, 4349.

(57) Gutsev, G. L.; Andrews, L.; Bauschlicher, C. W. *Theor. Chem. Acc.* **2003**, 109, 298.

(58) Bauschlicher, C. W.; Ricca, A. *J. Phys. Chem. A* **2002**, *106*, 3219.

(59) Wondimagegn, T.; Vanka, K.; Xu, Z.; Ziegler, T. *Organometallics* **2004**, *23*, 5737.

(60) Pandey, K. K.; Frenking, G. *Eur. J. Inorg. Chem.* **2004**, *22*, 4388.

(61) Gracia, L.; Andres, J.; Safont, V. S.; Beltran, A.; Sambrano, J. R. *Organometallics* **2004**, *23*, 730.

(62) Motta, A.; Lanza; G.; Fragala, I. L.; Marks, T. J. *Organometallics* **2004**, *23*, 4097.

(63) Pandey, K. K.; Lein, M.; Frenking, G. *Organometallics* **2004**, *23*, 2944.

(64) Møller, C.; Plesset, M. S. *Phys. Rev.* **1934**, *46*, 618.

(65) Head-Gordon, M.; Rico, R. J.; Oumi, M.; Lee, T. J. *Chem. Phys. Lett.* **1994**, *219*, 21.

(66) Mitin, A. V.; Baker, J.; Pulay, P. *J. Chem. Phys.* **2003**, *118*, 7775.

(67) Wachters, J. H. *J. Chem. Phys.* **1970**, *52*, 1033; Hay, P. *J. Chem. Phys.* **1977**, *67*, 4377.

(68) Bauschlicher, C. W. *Theor. Chim. Acta* **1995**, *92*, 183.

(69) Frisch, M. J.; Trucks, G. W.; Schlegel, H. B.; Scuseria, G. E.; Robb, M. A.; Cheeseman, J. R.; Montgomery, Jr., J. A.; Vreven, T.; Kudin, K. N.; Burant, J. C.; Millam, J. M.; Iyengar, S. S.; Tomasi, J.; Barone, V.; Mennucci, B.; Cossi, M.; Scalmani, G.; Rega, N.; Petersson, G. A.; Nakatsuji, H.; Hada, M.; Ehara, M.; Toyota, K.; Fukuda, R.; Hasegawa, J.; Ishida, M.; Nakajima, T.; Honda, Y.; Kitao, O.; Nakai, H.; Klene, M.; Li, X.; Knox, J. E.; Hratchian, H. P.; Cross, J. B.; Bakken, V.; Adamo, C.; Jaramillo, J.; Gomperts, R.; Stratmann, R. E.; Yazyev, O.; Austin, A. J.; Cammi, R.; Pomelli, C.; Ochterski, J. W.; Ayala, P. Y.; Morokuma, K.; Voth, G. A.; Salvador, P.; Dannenberg, J. J.; Zakrzewski, V. G.; Dapprich, S.; Daniels, A. D.; Strain, M. C.; Farkas, O.; Malick, D. K.; Rabuck, A. D.; Raghavachari, K.; Foresman, J. B.; Ortiz, J. V.; Cui, Q.; Baboul, A. G.; Clifford, S.; Cioslowski, J.; Stefanov, B. B.; Liu, G.; Liashenko, A.; Piskorz, P.; Komaromi, I.; Martin, R. L.; Fox, D. J.; Keith, T.; Al-Laham, M. A.; Peng, C. Y.; Nanayakkara, A.; Challacombe, M.; Gill, P. M. W.; Johnson, B.; Chen, W.; Wong, M. W.; Gonzalez, C.; Pople, J. A. *Gaussian 03*, Revision C.02; Gaussian, Inc., Wallingford CT, 2004.

(70) Becke, A. D. *J. Chem. Phys.* **1993**, *98*, 5648.

(71) Grotjahn, D. B.; Halfen, D. T.; Ziurys, L. M.; Cooksy, A. L. *J. Am. Chem. Soc.* **2004**, *126*, 12621.

(72) Kalemos, A.; Mavridis, A.; Harrison, J. F. *J. Phys. Chem. A* **2001**, *105*, 755.

(73) Ricca, A.; Bauschlicher, C. W. *Chem. Phys. Lett.* **1995**, *245*, 150.

(74) Hehre, W. J.; Ditchfield, R.; Pople, J. A. *J. Chem. Phys.* **1972**, *56*, 41.

(75) Dunning, T. H. *J. Chem. Phys.* **1989**, *90*, 1007.

(76) Becke, A. D.; Edgecombe, K. E. *J. Chem. Phys.* **1990**, *92*, 5397.

(77) Noury, S.; Krokidis, X.; Guster, F.; Silvi, B. *Comput. Chem.* **1999**, *23*, 597.

(78) Raub, S.; Jansen, G. *Theor. Chem. Acc.* **2001**, *106*, 223.

(79) Biegler-König, F. W.; Bader, R. F. W.; Tang, T. H. *J. Comput. Chem.* **1982**, *3*, 317.

(80) Noury, S.; Krokidis, X.; Fuster, F.; Silvi, B. *ToPMoD*; Laboratoire de Chimie Théorique, Université Pierre et Marie Curie: Paris, 1999.

(81) *MORPHY98*, a program written by P. L. A. Popelier with a contribution from R. G. A. Bone; UMIST: Manchester, England, 1998.

(82) Fradera, X.; Austen, M. A.; Bader, R. F. W. *J. Phys. Chem. A* **1999**, *103*, 304.

(83) Scherer, W.; McGrady, G. S. *Angew. Chem., Int. Ed.* **2004**, *43*, 1782.